Austin Journal of Radiology

Open Access

Austin Publishing Group

Research Article

Evaluating the Prevent Effect of Human Papillomavirus 16E7 Peptide-Based Therapeutic Vaccine Utilizing an Orthotopic TC-1 Cervical Tumour Model by 3.0T Magnetic Resonance Imaging in Mice

He XH[1], Chen YH[2], Huang LW[1], Zhou XH[1], Ni GY[3,4], Wang TF[3,4], Shelley W[4], Liu XS[2,3,4], Chen S[2]* and Gao MY[1]*

[1]Department of Medical Imaging, The First People's Hospital of Foshan, Foshan528000, Guangdong, China

[2]Cancer Research Institute, The First People's Hospital of Foshan, Foshan528000, Guangdong, China

[3]The first affiliated hospital/Clinical Medical School, Guangdong Pharmaceutical University, Guangzhou 528458, Guangdong, China

[4]Inflammation and Healing Research Cluster, University of Sunshine Coast, Maroochydore DC, QLD 4558, Australia

***Corresponding author:** Ming Yong Gao, Department of Medical Imaging, The First People's Hospital of Foshan, No.81 Lingnandadaobei, Chancheng District, Foshan City 528000, Guangdong Provence, China

Shu Chen, Cancer Research Institute, The First People's Hospital of Foshan, No.81 Lingnandadaobei, Chancheng District, Foshan City 528000, Guangdong Provence, China

Received: February 27, 2020; **Accepted:** April 10, 2020; **Published:** April 17, 2020

Abstract

The goal of this paper is to investigate whether a 3.0T magnetic resonance scanner with a small animal coil can monitor the orthotopic TC-1 cell Cervical Tumour (CT) growth in mice, and to evaluate the tumour growth prevent effect of Human Papillomavirus (HPV)16E7 peptide-based therapeutic vaccine. The TC-1 cells were implanted into cervical cavity of 52 female C57BL/6J mice (6 experiments), and followed by subcutaneously immunization of HPV16E7 peptide-based with interleukin 10 receptor antibody in 18 mice (3 groups) to observe the efficacy of the therapeutic vaccine. The same Magnetic Resonance Imaging (MRI) equipment and protocols were performed through the entire experiments. Images of each tumour-bearing mice were compared with blank mice to determine when the CTs can be determined by MRI. The Tumour Volume (TV) of each mice was monitored including 3 contrast enhanced tumors. The TV changes were evaluated by comparing the size on the same coronal MR images, and Signal Intensity (SI) measurement was adopted on 6 mice to predict the tumour growth trend. This study showed that the average CTs success rate was 90.38% (47/52), the tumour could be clearly detected on average 10 days. The maximum average SI values of tumour-bearing mice on day 4 was 2447, which was significantly higher than that of the blank mice, and increasing from day4 to day12. This study concluded that clinical 3.0T MRI scanner with small animal coil can be used to monitor the CTs, and to evaluate the CTs growth inhibitory effect of HPV16E7 peptide-based therapeutic vaccine, SI values may be used to predict cervical tumour growth and reliable than visual observation of early tumour images.

Keywords: Orthotopic cervical tumour model; TC-1 cell; Magnetic resonance imaging; Peptide-based vaccine; Therapeutic vaccine; Human papillomavirus

Abbreviations

CT: Cervical Tumour; HPV: Human Papillomavirus; MRI: Magnetic Resonance Imaging; TV: Tumour Volume; SI: Signal Intensity; PBS: Phosphate-Buffered Solution; CTL: Cytotoxic T Lymphocyte; IL-10: Blocking Interleukin 10; SPF: Specific Pathogen Free; FCS: Fetal Calf Serum; Gd-DTPA: Gadolinium Diethylene-Triamine Penta-Acetic Acid; HE: Hematoxylin-Eosin; SNR: Signal-To-Noise Ratio;

Introduction

Cervical cancer is one of the most common cancers in women worldwide, and is associated with continued infection of HPV16 and 18 [1]. Therapeutic vaccines, through the induction of Cytotoxic T Lymphocyte (CTLs), specifically kill tumour cells without obvious damage to normal cells and tissues; have become a research hotspot [2]. Previously, it was demonstrated that blocking Interleukin 10 (IL-10) signaling at the time of immunization drastically increase the vaccine induced CTL responses compared with the same vaccine without IL-10 signaling blockade, and the vaccine is able to prevent tumour growth [3-5].

Currently, HPV therapeutic vaccines are usually tested in mice models of HPV16E6/E7 transformed TC-1 tumour cells subcutaneously implanted into mice flank [6,7]. HPV16 transgenic mice model where HPV16E7 is expressed under the keratin 14 promoter is also used to study HPV16 induced epithelial tumour pathogenesis and the efficacy of therapeutic vaccines [8,9]. Although HPV therapeutic vaccines effectively inhibit tumour growth in mice, but they often have poor effect in the clinical trials of HPV-associated pre-cancer and cervical cancer [10,11].

HPV-associated tumours are mostly restricted to the genital mucosa. Regression of these tumours may require the induction of the effector T cell with mucosal homing signal or activation of a vaccine induced immune response in the local mucosal region [12,13]. Chronic exposure of estrogen is able to induce vaginal and cervical squamous carcinogenesis of HPV16 transgenic mice [14-16]. Similarly, orthotopic TC-1 mice model was also established by

Chen and Gao et al. © All rights reserved

Citation: He XH, Chen YH, Huang LW, Zhou XH, Ni GY, Wang TF, et al. Evaluating the Prevent Effect of Human Papillomavirus 16E7 Peptide-Based Therapeutic Vaccine Utilizing an Orthotopic TC-1 Cervical Tumour Model by 3.0T Magnetic Resonance Imaging in Mice. Austin J Radiol. 2020; 7(1): 1106.

different groups through injection of medroxyroprogest nonoxynol-9 intra-vaginally before tumour challenge [17,18].

Magnetic Resonance Imaging (MRI) is a common approach to demonstrate the tumour and its surrounding tissues [19,20]. MRI has high special resolution and high contrast of soft tissue. It also provides a non-invasive way to observe the growth of tumour or estimate the impact of intervention. This approach is now even possible to detect circulating tumour cells [21]. As a non-invasive imaging technique, MRI has several advantages including an excellent soft tissue contrast in combination with the 3D acquisition of morphology and function. MRI has a high accuracy and excellent solution to diagnostic and staging tumour of the cervix [22].

To assess the efficacy of a HPV therapeutic vaccine containing IL-10 signaling inhibitor in a more relevant setting, in the current paper, we established an orthotopic intra-vaginal HPV16 E6/E7 transformed TC-1 cell tumour mice model, and evaluated the anti-tumour effect of a HPV16E7 peptide-based therapeutic vaccine using a clinical 3.0T MR scanner supplemented with a small animal coil.

Materials and Methods

Mice

Six to eight weeks old female C57BL/6J mice were purchased from animal experiment center of Guangzhou, Guangdong province, China. The mice were housed under Specific Pathogen Free (SPF) conditions and used according to the recommendations for the proper use and care of laboratory animals. All mice were kept at SPF condition on a 12-hr light/12-hr dark cycle. The temperature of the animal house was 22°C and the humidity was 75%. 5 mice were kept each cage, provided with sterilized standard mouse food and water. Mice were sacrificed by CO_2 inhalation at the end of each experiment and confirmed by the ceasing of heart beat. Body condition scoring was used to monitor the health of tumour-bearing mice [23].

Cell line

TC-1 cells were bought from Chinese academy of sciences, Shanghai institutes of cell resource center, and maintained in RPMI 1640 media (Gibco, USA) supplemented with 10% heat inactivated Fetal Calf Serum (FCS), 100U of penicillin/ml and 100μg of streptomycin/ml in the presence of G418 at 0.4 mg/ml and cultured at 37°C with 5% CO_2 as described elsewhere [5].

Peptides and reagent

HPV16E7 overlapping peptide (ME, CP, DR, LC) were synthesized and purified by Mimotopes (Wuxi, China).

ME sequences:

MHGDTPTLHEYMLDLQPETTDLYCYEQLNDSSEEE.

CP sequences:

LNDSSEEEDEIDGPAGQAEPDRAHYNIVTFCCKC.

DR sequences: DRAHYNIVTFCCKCDSTLRLCVQSTHVDIR.

LC sequences: CVQSTHVDIRTLEDLLMGTLGIVCPICSQKP.

Monophosphoryl Lipid A (MPLA) were obtained from sigma, USA. Anti-IL10 receptor (α-IL10R, clone: 1B1.3a) monoclonal antibody was purchased from BioXcell, USA, and stored at -70°C degree before use. Ex/MPLA/α-IL10R contains four E7 peptides, each 10μg; 15μg of MPLA and 300μg of α-IL10R antibody in 100μl of PBS.

Ex/MPLA contains four E7 peptides, each 10μg; 15μg of MPLA in 100μl of PBS.

Medroxyprogesterone (Med Chem Express, USA); Nonoxynol-9 (Sigma, USA) ; Carboxymethylcellulose (Sigma, USA); PBS (Hyclone, USA).

MR scanner

Clinical 3.0T MR system (Model: GE Discovery 750w (GE Healthcare, Waukehsa, USA) and a 4-channel receive only small animal RF coil (Model: WK602, SN: 1236, Magtron, Jiangyi, China) were used. This coil was a standard accessory of the GE 3.0T MR system, and the coil was set to the head-imaging mode.

Establish orthotopic TC-1cell cervical tumour mice model

Mice were treated with 3 mg of medroxyprogesterone (Med Chem Express, USA) via subcutaneous injection. 3 days later, they were intra-vaginally given with 50μl of 4% nonoxynol-9 (Sigma, USA) diluted in 4% carboxymethylcellulose (Sigma, USA) overnight. On the next day, genital tract of each mice was washed with PBS (Hyclone, USA) before implanted with 1.5×10^5 of TC-1 cells into the cervical cavity through a plastic funnel. 8, 10, 13, 10, 6 and 5 in total 52 mice and 6 experiments were repeated, respectively.

Prevent tumour growth experiment

The same method as above was used to implanted the same 1.5×10^5 TC-1 cell into the cervix of another 18 mice. 3 days later, the 18 mice were divided into 3 groups on average and immunized subcutaneously with Ex/MPLA/α-IL10R, Ex/MPLA or PBS on the rear right leg twice 7 days apart, respectively.

All the TC-1 cells implanted procedures were performed under the mice anesthetic state by injecting 200μl of 4% chloral hydrate intra-peritoneally [24].

MR scan preparation

All the MR imaging mice were performed under anesthetic state as the same described above [24]. Each mice was prone to the small animal coil, and the midsagittal axis of mice was coincide with the coil long axis, while the transverse axis of mice was coincide with the coil short axis. For the blank mice, 60μL of 0.9% physiological saline was injected into its rectum, and a funnel was retained in its vaginal/cervical cavity and fixed with adhesive tape.

MR scan

The coil with the imaging mice was placed at the center of the MR scanner by laser guidance. MR scan was performed during the mice was stationary completely and free breathing. The earliest MR scan was day4 after the TC-1 cells were implanted. All MRI sequences were based on the clinically used in our department, this may potentially facilitate translation of imaging findings between rodent and human studies [25]. According to our pre-experiment experiences, 7 slices in coronal plane and a series 3D T1 images of each mice can meet the image analysis requirement. Thus, the scan sequences of this study included: (1) a low-resolution three plane scout sequence; (2) coronal plane fast spin echo T2 weighted (COR T2WI) sequence; (3) 3D T1 sequence (3D T1) and (4) contrast enhanced 3D T1(3D T1+C)

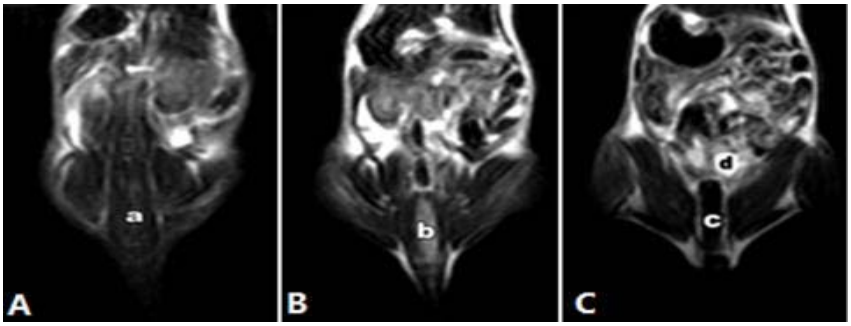

Figure 1: Coronal T2WI images of genital tract and its surrounding structure of C57BL/6J blank mice. **(A)** Letter a marks the mice spinal (spinal code). **(B)** Letter b marks the mice rectum with 60μL of 0.9% physiological saline injected into**. (C)** Letter c marks the location of a little funnel placed into the mice vagina/cervical cavity, and letter d marks the mice bladder.

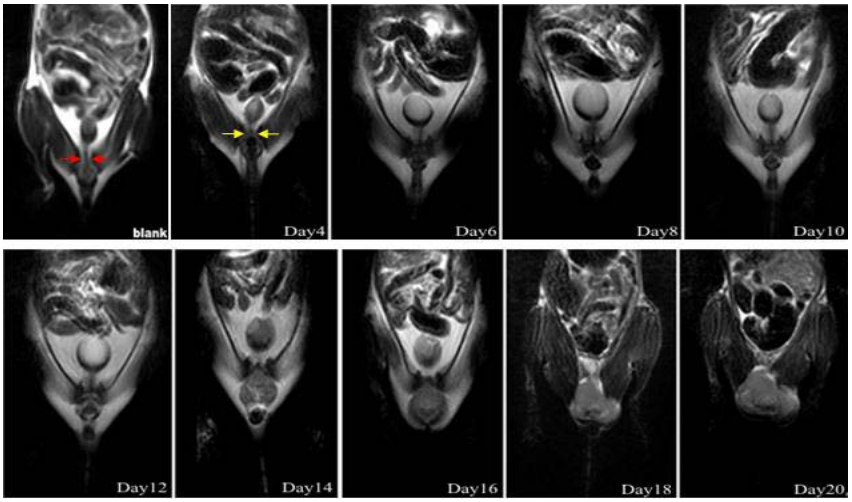

Figure 2: Coronal T2WI images of blank and tumour-bearing mice. The tumour-bearing mice genital tract (yellow arrows) was seen shorter and obvious expansion after TC-1 cells implanted compared to that of the blank one (red arrows).The same coronal image of the same tumour-bearing mice from Day 4 to Day 20 had shown the tumour growth process. The tumour could be identified clearly on Day 10's image.

sequence.

A low-resolution scout sequence (three-dimensional gradient echo sequence) was used to obtain an anatomical overview and target localization. The COR T2WI sequence was achieved by: Repetition Time (TR)=5130ms, Echo Time(TE)=130ms, Field Of View (FOV)=8.0, Phase FOV=0.6, Number of Excitation (NEX)=8, Acquisition Matrix (AM)=256×224 (read×phase), Slice Thickness (ST)=1.0mm, Thickness Space (TS)=0.5, Echo Train Length (ETL)=26, Intensity Filter (IF)=B, Shim=auto, Auto Refocus Angle (ARA)=111°, Receiver Bandwidth (RB)=10.0, Freq dir=S/I. The 3D T1 sequence was achieved by TR=18.0ms, TE=8.4ms, FOV=8.0, Phase FOV=0.80, NEX=2, AM=256×224, ST=1.0mm, RB=10.0, FA=15°, Prep time=450, IF=A, Shim=auto, Freq dir=S/I, Acceleration phase=1.50.

3 mice models were intravenously injected with 0.1mmol/kg of Gadolinium Diethylene-Triamine Penta-Acetic Acid (Gd-DTPA) from the tail vein after the 3D T1 sequence for the 3D T1+C sequence, and immediately achieved with the same protocols as 3D T1 above for a total of 3 times scan each mice.

MR images analysis

Source images were exported as DICOM files and analyzed on a GE ADW4.6 workstation by one researcher. The tumour volume was estimated by manually measuring the length, width and height on 3D T1 images.

The Signal density (SI) of each tumour was measured in the same genital tract region of each mice on the coronal images of 52 mice model and 18 tumour growth inhibit experiment mice. A rectangular ROI was placed under the bladder on coronal image, covering the vaginal/cervical cavity with an area of 19.3mm^2. The Maximum (Max), Mean (M) and Standard Deviation (SD) values of 3 slices were measured in each mice per time. The average values of the Max, M and SDs were recorded as the final SI of each mice per time respectively. SI measurement started at the same time of the first scan and finished at the same time when tumour was visible clearly.

The survival time was calculated based on the unit of day for the 52 mice model and 18 tumour growth inhibition experiment mice.

All the image visual evaluation was completed by two researchers independently, and the third researcher participated in the discussion to solve the different independent evaluation opinions, if necessary.

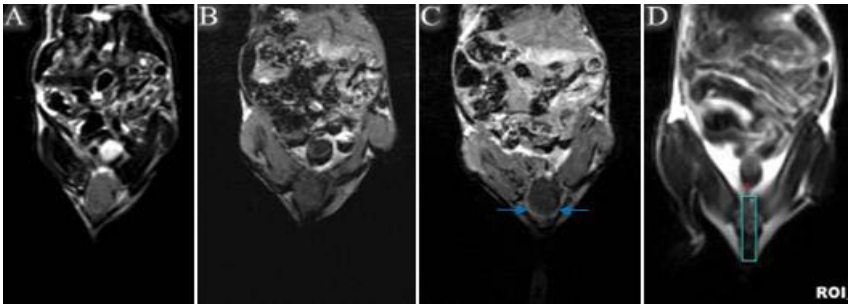

Figure 3: Non-contrast enhanced, contrast enhanced images and SI measurement ROI. **A** and **B** were the same slice of non-contrast enhanced T2 and T1 weighted coronal images from the same tumour-bearing mice. **C** was the same slice as A and B,Gd-DTPA enhanced and 5min delayed T1 weighted image, its tumour outline (blue arrows) clearer than that of the non-contrast enhanced**. D** was the SI measurement ROI of the mice vaginal/cervical cavity.

Pathology analysis

Genital tract tissues included vagina, cervix and the surrounding tissues were paraffin embedded, and then sectioned transversely, stained with Hematoxylin-Eosin (HE). 100× and 200× optical microscope was employed to observe genital tract and its surrounding tissues morphology of normal and tumour-bearing mice.

Results

Clinical 3.0T MR system with a small animal coil can monitor the growth of orthotopic TC-1 cell cervical tumour

Coronal T2WI images from normal mice were shown in Figure 1. The images were clear and have good soft tissue contrast, the spine (or spinal cord), rectum, vaginal/cervical cavity, bladder and tail of the normal mice were clearly distinguished. By comparing the images of blank (normal) and day4 images of mice challenged with TC-1 tumour (Figure 2), the genital tract with TC-1 cells was shorter and expanded than the blank one's. The tumour grew slowly in the early stage and most of them were recognized as little round soft tissue images located in the cervical cavity the 8th to 12th day after tumour cells challenged. The tumors grew rapidly along the genital tract, and gradually squeezed the surrounding tissues about 14 days later, most of tumour shapes were irregular, and the structures of rectum, vaginal/cervical cavity and bladder, as shown in Figure 1, could be difficult to be distinguished, some of the tumours even protruded vagina. At the later stage (20 days later), The tumour volumes and shapes were changed not significantly. Tumour internal signals were uniform and the edge was clear when the tumours were small. With the increase of tumour volume, inhomogeneous internal signals and necrosis areas could often be recognized; meanwhile the edge of tumours became blurred due to the tumours invading the adjacent tissues. Images from Day 4 to Day 20 on Figure 2 were the coronal T2WI images of the same mice showing that the tumour grew gradually, and tumour could be firstly identified clearly on Day 10 after tumour cells challenged.

Gd-DTPA contrast enhancement images better reflect the tumour border and nearby normal tissues

Coronal images of Figure 3(A,B,C) were from the same tumour-bearing mice. Compared with the (A) non-enhanced T2 weighted and (B) T1 weighted images, the tumour outline (blue arrows) became clearer on the Gd-DTPA enhanced T1 weighted image, although the internal mass of tumours no contrast enhanced (C).

SI values compared between blank and tumour-bearing mice

MRI signal is the electromagnetic wave with phase, frequency and intensity detected. The electromagnetic waves are processed and reconstructed to form MR images, reflecting the shape of the imaging object based on the characteristics and time sequences of different tissues.SI is actually the amount of signals that can be processed and reconstructed. In this study, due to the limitation of signal receiving and processing by MRI scanners, MR signals from the TC-1 cells were insufficient to reflect the CTs morphological characteristics at least 8 days after transplantation, therefore, the earlier CTs morphological changes couldn't be clearly observed on the corresponding MR images. However, these MR signal changes could be expressed in numbers or digitized directly. SI values in Table 1 were measured in the genital tract region (Figure 3D). The average SI value of day4 after TC-1cells challenged was significantly higher than that of the blank one's, and the SI values were increased gradually from day4 to day12, which suggested that SI values could be used as an earlier surrogate marker to predict the tumour growth by MRI in this study.

Successfully established orthotopic TC-1 cell cervical tumour mice model

Table 2 showed the success rate of mice model, which ranged from 75% to 100%, with an average of 90.38% (47/52), and it took an average of 10 days to clearly observe tumour on coronal MR images, and the average survival time of the tumour-bearing mice was 25.3 days. The genital tracts and its surrounding structures between the normal and tumour-bearing mice were obvious different under the microscopy (Figure 4). It could be seen that there was no clear border between the tumour and the genital tract wall of the tumour-bearing mice, tumour cells invaded the submucosa of the vagina/cervix, and truly imitated the biological behavior of human cervical cancer (C, D).

Therapeutic vaccine prevents orthopedic TC-1 tumour growth

We investigated whether HPV16E7 peptide-based therapeutic vaccine is able to prevent orthopedic cervical TC-1 tumour growth. Figure 5 showed tumour volumes obtained by MR scanning of 3 different groups of subcutaneously immunized tumour-bearing mice. The maximum tumour volume of mice with Ex/MPLA/α-IL10R immunized was average 684.28mm^3, which was significantly smaller than that of 1350.54mm^3 (Ex/MPLA group) and 1518.50mm^3 (PBS

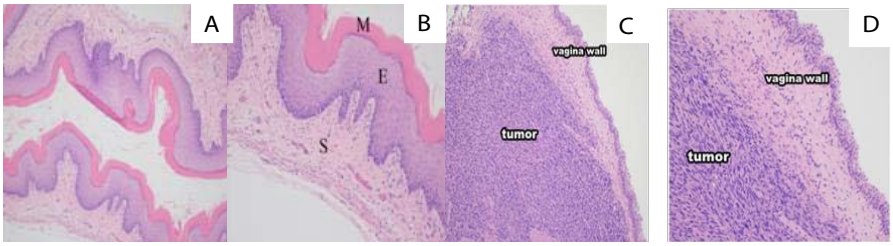

Figure 4: Normal and tumour-bearing mice genital tract and its surrounding tissues under optical microscope. **(A)** Normal mice, 4-um transversal sections obtained from one of the blank mice, ×100 magnification; **(B)** The same section as **(A)**, ×200 magnification (M: Mucosa, E:Epithelium, S: Stroma). It could be seen that there was very clear border between different tissues of the normal genital tract wall; **(C)** tumour-bearing mice, 4-um transversal serial sections obtained from one of the tumour-bearing mice, ×100 magnification; **(D)** the same section as **(C)**, ×200 magnification. It could be seen that there was no clear border between the tumour and the genital tract wall.

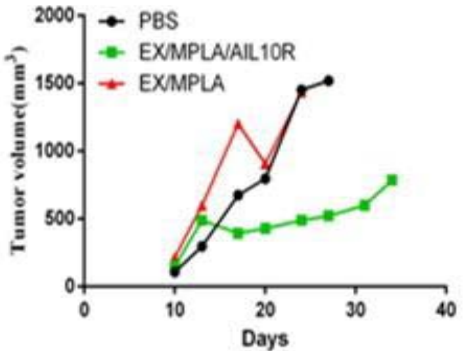

Figure 5: Mice tumour volume of 3 groups of subcutaneously immunized prevent tumour growth experiment. The maximum tumour volume of mice with Ex/MPLA/α-IL10R immunized group was obviously smaller than that of Ex/MPLA or PBS groups, while there was no difference between the Ex/MPLA and PBS groups.

group) respectively, while there was no difference between Ex/MPLA and PBS groups.

Discussion

In this study, we successfully established the orthotopic cervical tumour models in C57BL/6 mice by implanting the TC-1 cell into the cervical cavity, and successfully monitored the tumour growth on a clinical 3.0T MR system with a small animal coil. It took an average of 10 days to observe clearly the tumours on the coronal MR images. The average success rate was 90.38% (47/52, Table 2), and the average survival time of the 52 mice was 25.3 days. The maximum tumour volumes were different among the 3 groups of the subcutaneously immunized prevent tumour growth experiments, which indicated that the HPV16E7 peptide-based therapeutic vaccine might be used to prevent the cervical tumour growth and worth further investigation.

The subcutaneous transplanted tumours were usually observed and monitored by the local changes of implantation site. However, orthotopic tumour models mimic better than subcutaneously transplanted tumour models, and usually require using imaging equipments to monitor. Similar to the model of hepatocellular carcinoma in mice, the orthotopic cervical tumour models can also be monitored by using high-frequency ultrasound. But the result judgments are closely related to the experience of the ultrasound operators. Another way was to make the tumour cells to express luciferase or green fluorescent protein and detect subsequent the

Table 1: SI in genital tract ROIs of the blank (n=1) and tumour-bearing mice (n=6).

	blank	day 4	day 6	day 8	day 10	day 12
Maximum	993	2447	2734	2980	3253	3512
Mean	371	890	975	1053	1073	1573
Standard deviation	213.5	557.75	528.57	567.14	516.5	712.38

Note: SI = Signal Intensity. Original data of the tumour-bearing mice corresponded to Experiment 5 in Table 2. The values corresponding to blank were the average of two times measured; Maximum, Mean and Standard deviation values were the average values of the 6 tumour-bearing mice.

Table 2: MRI confirmed orthotopic TC-1cell cervical tumour mice model success ratio.

	n	TI	NTI	FTTI	SR (%)
Experiment 1	8	6	2	10	6/8(75.00)
Experiment 2	10	10	0	8	10/10(100.00)
Experiment 3	13	12	1	10	12/13(92.31)
Experiment 4	10	9	1	10	9/10(90.00)
Experiment 5	6	6	0	10	6/6(100.00)
Experiment 6	5	4	1	12	4/5(80.00)
Average				10	47/52(90.38)

Note: n = number of samples; TI = Tumour Identified; NTI = No Tumour Identified; FTTI = First Time Tumour Identified; SR = Success Ratio

signaling strength luciferase or fluorescence. However, the methods mentioned above had common features of lacking accurate cervical anatomical position simulation and observation of its surrounding structure, as well as intuitive identification of tumour internal structure. With the advantages of non-ionizing radiation harm, multi-sequence and multi-parameter scanning, excellent soft tissue resolution, visual and readable images, MRI technology plays an increasing important role in the living animal models researches.

In terms of monitoring the orthotopic cervical tumour growth, it is ideal to use ultra-high field strength (4.7–16.4T) special MRI equipment. However, most of clinical medical institutions lack such equipment. The clinical 1.5T or 3.0T MRI systems with a clinical wrist or other microscopy coils [25-31], and home-build birdcage radio frequency coil [32] or customized transmit/receive volume coil [33] were demonstrated to be effectively used for small living animal imaging researches. These reports indicated that instead of ultra-high field strength MRI scanner, the clinical MRI scanners are also the valuable selection for this kind of investigations. However, due to the limitations of the lower magnet field strength (1.5–3.0T)

and larger coils used, clinical MRI scanners commonly yield a lower Signal-to-Noise Ratio (SNR) and poorer spatial resolution when used for small animal studies, compared to the dedicate scanners with the field strength of 4.7–16.4T ones [25].

Based on the aim of improving the SNR and spatial resolution, a small animal coil that can be connected to the clinical MRI systems has been reported to contribute to similar investigations of mice models [34]. Our results also showed that the clinical 3.0T MR system equipped with a special 4-channel receiving only small animal coil can effectively perform MRI of mice model, and the image quality is suitable enough to distinguish the genital tract and its surrounding structure of C57BL/6 mouse. In order to help researchers to accurately and quickly locate the relative position of genital tract and the surrounding structures of mice correctly on images, a small funnel which used for transplanting TC-1 cells was fixed in the vaginal cavity of the blank mice before scanning (Figure 1). Coronal T2-weighted images were obtained from day4 to day20, with 2 days interval each time after tumour cells were implanted by using the same scanning equipment and protocols. The MRI image of the genital tract region was different between the tumour-bearing mice (Figure 2, yellow arrows) and the blank mice (Figure 2, red arrows). We believe that these early (day4) image characteristic differences indicate that the TC-1 cells have been implanted into the right place of the mice and began to grow, which then led to cervical cavity dilatation of tumour-bearing mice. Previous reports have shown that the first imaging time is about 7 days after tumor inoculation using a 9.4T horizontal hole small animal MR scanner equipped with a 25mm serrated resonator [35]. In this study, although very few tumorus can be clearly observed on the 8th day, the vast majority of tumorus can't be clearly identified until the 10th day. This shows that the first scanning time of mice with clinical 3.0T MRI system connected with small animal coil should not be earlier than the 8th or 10th day after TC-1 cell implantation, which is later than that of special MRI system for small animals. This difference is mainly due to the higher SNR and spatial resolution of the ultra-high field strength system than the clinical 3.0T system.

Theoretically, when detected MRI signal is enough to reflect the morphological change between the tumour tissue and the adjacent tissues, the differences can be identified subjectively on the images. However, the image reproduction and subjective recognition ability of this tissue contrast difference is affected by the performance of the instrument and the subjective consciousness of the image reader. In terms of the cervical tumor model established in this study, it can be clearly identified on the MR image only depended on the surviving TC-1 cells and continue to grow for about 10 days after transplanted into the cervical cavity. This is a "long" waiting duration for some researches that need to judge the success or failure of model establishment quickly. But in essence, the difference of MR signal between tumour and adjacent tissue structure is a consecutive process from quantitative change to qualitative change. In other words, the gradual visibility caused by tumour morphological changes is a dynamic process, which is based on the synchronous enhancement of MRI signals in corresponding regions created by the increasing tumour cells, and the formation of morphological differences through sufficient MRI signals. Other than MRI signals can be reconstructed images for visual identification, the dynamic evolution process of MRI signals created by local tissues can also be quantified by ROI or other technologies to analyze the micro-elements of image composition details, and displayed in digital quantitative or semi quantitative way. Therefore, by using ROI analysis technology, we can monitor the changes of MRI signal intensity in the same ROI before the visible changes of tumor morphology, so as to predict the growth rate and development trend of tumours.

The results of this study showed that by monitoring the SI value of cervical ROI after TC-1 cell transplantation and comparing with that of the blank mice, obvious differences have been showed on the image of day4, and SIs showed the consecutive rising trend from the later monitoring data until the tumour could be clearly observed meanwhile the measurement terminated, as shown in Table 1.

This result indicated that although the ultra-high field strength system has obvious advantages in image reproduction compared with the clinical 3.0T system, if the ROI quantitative or semi quantitative analysis method is used, both of them may have similar ability to predict the model establishment earlier. However, for the vast majority of medical institutions, the cost performance of clinical 3.0T MR system with small animal coil is much higher than that of ultra-high field strength MR system. Similarly, SI values monitoring with ROI technology can also help to evaluate the early response of tumor to various treatment methods before the visible morphological changes of image, and help to predict the curative effect and the revision of treatment plan. Therefore, the objective results of high sensitivity and accuracy could also be obtained through the right methods and technologies, even if low-end equipment is used.

Previous researches have described the data acquisition of contrast enhanced MRI from tumour-bearing mice on clinical scanners [25,28-30], and the enhancement peak was at half minute and gradually declined thereafter in mice in the Gd-DTPA enhancement study [25], it may be related to the characteristics of "fast uptake and fast wash-out" of malignant tumours after contrast agent injected. According to our results, contrast enhanced imaging could show the contours of tumours more clearly duo to improve the contrast between the tumour and its surrounding structures (Figure 3A,B,C). This may help to reveal smaller tumours than that without contrast enhancement, or to find tumours earlier. Due to the limitation of experimental conditions, the dynamic perfusion scanning mode did not use in this study, and the general interval was one minute at least from the completion of contrast agent injected to the beginning of scan, missed the peak time of contrast agent staying in tumour, and that was why the internal mass of tumours no contrast enhanced in this study.

Previously, we demonstrated that blocking IL-10 at the time of immunization drastically increase the vaccine induced T cell responses and inhibit transplanted TC-1 tumour growth [5]. In this study, using the orthotopic TC-1 cell cervical tumour model, a similar result was obtained (Figure 5), suggesting this orthotopic model could be used for the therapeutic vaccine efficacy research. It would be very interesting to investigate whether, in a therapeutic setting, this vaccine candidate is effective against orthopedic TC-1 cervical tumour. These results may reflect whether T cells may require mucosal homing signal for effective killing cervical tumour. We are currently investigating whether cervical tumour infiltrating T cells are different from those infiltrating the conventional transplanted

TC-1 tumour using the same orthotopic mice model as this study.

Conclusion

This study showed that the clinical 3.0T MR scanner with a small animal coil can be used to monitor the orthotopic cervical tumour growth, and to evaluate the cervical tumour growth inhibitory effect of HPV16E7 peptide-based therapeutic vaccine. SI values may be more sensitive than the visual observation of a tumour by MR scanning.

Funding

This work was partially funded by Science and Technology Research program of Foshan city (2018AB003471, 2012AA100461 and FS0AA-KJ218-1301-0039), Foshan City Council Research Platform Fund (2015AG1003), National Natural Science Foundation of China (81472451), Science and Technology Research program of Guangdong province (2016A020213001 and 2012B03180003).

Contributions

All authors have made substantial contributions to conception and design (He XH, Liu XS, Chen S, Gao MY), acquisition and analysis of data (Chen YH, Huang LW, Zhou XH), or analysis and interpretation of data (He HX, Ni GY, Wang TF, Shelley W); all were involved in drafting the article or revising it critically for important intellectual content; and all gave final approval.

References

1. Stanley M. Preventing cervical cancer and genital warts-How much protection is enough for HPV vaccines?. J Infect. 2016; 72: S23-28.
2. Ring KL, Yemelyanova AV, Soliman PT, Frumovitz MM, Jazaeri AA. Potential immunotherapy targets in recurrent cervical cancer. Gynecol Oncol. 2017; 145: 462-468.
3. Ni G, Wang T, Walton S, Zhu B, Chen S, Wu X, et al. Manipulating IL-10 signaling blockade for better immunotherapy. Cell Immunol. 2015; 293: 126-129.
4. Liu XS, Y Xu, Hardy L, Khammanivong V, Zhao W, Fernando GJ, et al. IL-10 mediates suppression of the CD8 T cell IFN-gamma response to a novel viral epitope in a primed host. J Immunol. 2003; 171: 4765-4772.
5. Chen S, Ni G, Wu X, Zhu B, Liao Z, Wang Y, et al. Blocking IL-10 signaling at the time of immunization renders the tumour more accessible to T cell infiltration in mice. Cell Immunol. 2016; 300: 9-17.
6. Wick DA, Webb JR. A novel, broad spectrum therapeutic HPV vaccine targeting the E7 proteins of HPV16, 18, 31, 45 and 52 that elicits potent E7-specific CD8T cell immunity and regression of large, established, E7-expressing TC-1 tumours. Vaccine. 2011; 29: 7857-7866.
7. Chen S, Wang X, Wu X, Wei MQ, Zhang B, Liu X, et al. IL-10 signalling blockade at the time of immunization inhibits Human papillomavirus 16 E7 transformed TC-1 tumour cells growth in mice. Cell Immunol. 2014; 290: 145-151.
8. Araújo R, Santos JMO, Fernandes M, Dias F, Sousa H, Ribeiro J, et al. Expression profile of microRNA-146a along HPV-induced multistep carcinogenesis: a study in HPV16 transgenic mice. J Cancer Res Clin Oncol. 2018; 144: 241-248.
9. Santos C, Ferreirinha P, Sousa H, Ribeiro J, Bastos MM, Neto T, et al. Ptaquiloside from bracken (Pteridium spp.) inhibits tumour-infiltrating $CD8^+$ T cells in HPV-16 transgenic mice. Food Chem Toxicol. 2016; 97: 277-285.
10. Chen J, Ni G, Liu XS. Papillomavirus virus like particle-based therapeutic vaccine against human papillomavirus infection related diseases:immunological problems and future directions. Cell Immunol. 2011; 269: 5-9.
11. Bergot AS, Kassianos A, Frazer IH, Mittal D. New Approaches to Immunotherapy for HPV Associated Cancers. Cancers (Basel). 2011; 3: 3461-3495.
12. Maldonado L, Teague JE, Morrow MP, Jotova I, Wu TC, Wang C, et al. Intramuscular therapeutic vaccination targeting HPV16 induces T cell responses that localize in mucosal lesions. Sci Transl Med. 2014; 6: 221ra13.
13. Sandoval F, Terme M, Nizard M, Badoual C, Bureau MF, Freyburger L, et al. Mucosal imprinting of vaccine-induced $CD8^+$ T cells is crucial to inhibit the growth of mucosal tumours. Sci Transl Med. 2013; 5: 172ra20.
14. Arbeit JM, Howley PM, Hanahan D. Chronic estrogen-induced cervical and vaginal squamous carcinogenesis in human papillomavirus type 16 transgenic mice. Proc Natl Acad Sci U S A. 1996; 93: 2930-2935.
15. Sepkovic DW, Raucci L, Stein J, Carlisle AD, Auborn K, Ksieski HB, et al. 3,3'-Diindolylmethane increases serum interferon-gamma levels in the K14-HPV16 transgenic mouse model for cervical cancer. *In Vivo*. 2012; 26: 207-211.
16. Garbow JR, Santeford AC, Anderson JR, Engelbach JA, Arbeit JM. Magnetic resonance imaging defines cervicovaginal anatomy, cancer, and VEGF trap antiangiogenic efficacy in estrogen-treated K14-HPV16 transgenic mice. Cancer Res. 2009; 69: 7945-7952.
17. Soong RS, Song L, Trieu J, Knoff J, He L, Tsai YC, et al. Toll-like receptor agonist imiquimod facilitates antigen-specific $CD8^+$ T-cell accumulation in the genital tract leading to tumour control through IFNγ. Clin Cancer Res. 2014; 20: 5456-5467.
18. Zeng Q, Peng S, Monie A, Yang M, Pang X, Hung CF, et al. Control of cervicovaginal HPV-16 E7-expressing tumours by the combination of therapeutic HPV vaccination and vascular disrupting agents. Hum Gene Ther, 2011; 22: 809-819.
19. Zheng L, Zhang Z, Khazaie K, Saha S, Lewandowski RJ, Zhang G, et al. MRI-monitored intra-tumoural injection of iron-oxide labeled Clostridium novyi-NT anaerobes in pancreatic carcinoma mouse model. PloS One, 2014; 9: e116204.
20. Dappa E, Elger T, Hasenburg A, Düber C, Battista MJ, Hötker AM. The value of advanced MRI techniques in the assessment of cervical cancer: a review. Insights Imaging. 2017; 8: 471-481.
21. Castro CM, Ghazani AA, Chung J, Shao H, Issadore D, Yoon TJ, et al. Miniaturized nuclear magnetic resonance platform for detection and profiling of circulating tumour cells. Lab Chip. 2014; 14: 14-23.
22. Dhoot NM, Kumar V, Shinagare A, Kataki AC, Barmon D, Bhuyan U. Evaluation of carcinoma cervix using magnetic resonance imaging: correlation with clinical FIGO staging and impact on management. J Med Imaging Radiat Oncol. 2012; 56: 58-65.
23. Ullman-Cullere MH, Foltz CJ. Body condition scoring: a rapid and accurate method for assessing health status in mice. Lab Anim Sci. 1999; 49: 319-323.
24. Decrausaz L, Goncalves AR, Domingos-Pereira S, Pythoud C, Stehle JC, Schiller J, et al. A novel mucosal orthotopic murine model of human papillomavirus-associated genital cancers. Int J Cancer. 2011; 128: 2105-2113.
25. Jansen CHP, Reimann C, Brangsch J, Botnar RM, Makowski MR. *In vivo* MR-angiography for the assessment of aortic aneurysms in an experimental mouse modelon a clinical MRI scanner: Comparison with high-frequency ultrasound and histology. PLoS One. 2017; 12: e0178682.
26. Jogiya R, Makowski M, Phinikaridou A, Patel AS, Jansen C, Zarinabad N, et al. Hyperemic stress myocardial perfusion cardiovascular magnetic resonance in mice at 3 Tesla:initial experience and validation against microspheres. J Cardiovasc Magn Reson. 2013; 15: 62.
27. Ferguson PM, Slocombe A, Tilley RD, Hermans IF. Using magnetic resonance imaging to evaluate dendritic cell-based vaccination. PLoS One. 2013; 8: e65318.
28. Egeland TA, Simonsen TG, Gaustad JV, Gulliksrud K, Ellingsen C, Rofstad EK. Dynamic contrast-enhanced magnetic resonance imaging of tumours:preclinical validation of parametric images. Radiat Res. 2009; 172: 339-347.

29. Hompland T, Ellingsen C, Rofstad EK. Preclinical evaluation of Gd-DTPA and gadomelitol as contrast agents in DCE-MRI of cervical carcinoma interstitial fluid pressure. BMC Cancer. 2012; 12: 544.

30. Eriksson PO, Aaltonen E, Petoral R Jr, Lauritzson P, Miyazaki H, Pietras K, et al. Novel nanosized MR contrast agent mediates strong tumour contrast enhancement in an oncogene-driven breast cancer model. PLoS One. 2014; 9: e107762.

31. Botnar RM, Brangsch J, Reimann C, Janssen CHP, Razavi R, Hamm B, et al. *In vivo* molecular characterization of abdominal aortic aneurysms using fibrin-specific magnetic resonance imaging. J Am Heart Assoc. 2018; 7: e007909.

32. Hong GB, Zhou JX, Yuan RX. Folate-targeted polymeric micelles loaded with ultrasmall superpara magnetic iron oxide: combined small size and high MRI sensitivity. Int J Nanomedicine. 2012; 7: 2863-2872.

33. Kuo YT, Chen CY, Liu GC, Wang YM. Development of bifunctional gadolinium-labeled superparamagnetic nanoparticles (Gd-MnMEIO) for *In vivo* MR Imaging of the liver in an animal model. PLoS One. 2016; 11: e0148695.

34. Guo Q, Liu Y, Xu K, Ren K, Sun W. Mouse lymphatic endothelial cell targeted probes: anti-LYVE-1 antibody-based magnetic nanoparticles. Int J Nanomedicine. 2013; 8: 2273-2284.

35. Yang M, Yu T, Wang YY, Lai SK, Zeng Q, Miao B, et al. Vaginal delivery of paclitaxel via nanoparticles with non-mucoadhesive surfaces suppresses cervical tumour growth. Adv Healthc Mater. 2014; 3: 1044-1052.